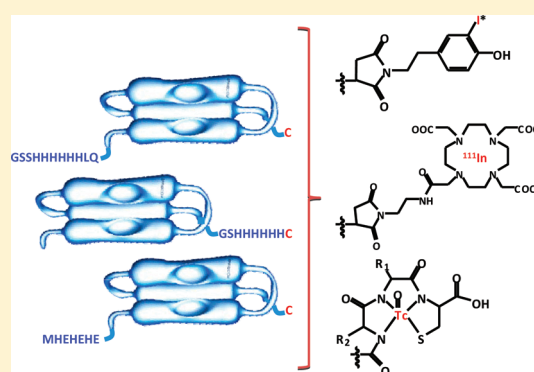


Use of a HEHEHE Purification Tag Instead of a Hexahistidine Tag Improves Biodistribution of Affibody Molecules Site-Specifically Labeled with ^{99m}Tc , ^{111}In , and ^{125}I Camilla Hofström,[†] Anna Orlova,[‡] Mohamed Altai,[‡] Fredrik Wängsell,[§] Torbjörn Gräslund,[†] and Vladimir Tolmachev^{*,‡}[†]Department of Molecular Biotechnology, Royal Institute of Technology, Stockholm, Sweden[‡]Division of Biomedical Radiation Sciences, Rudbeck Laboratory, Uppsala University, Uppsala, Sweden[§]Department of Medicinal Chemistry, Organic Pharmaceutical Chemistry, Uppsala University, Uppsala, Sweden

ABSTRACT: Affibody molecules are a class of small (~7 kDa) robust scaffold proteins suitable for radionuclide molecular imaging in vivo. The attachment of a hexahistidine (His₆)-tag to the Affibody molecule allows facile purification by immobilized metal ion affinity chromatography (IMAC) but leads to high accumulation of radioactivity in the liver. Earlier, we have demonstrated that replacement of the His₆-tag with the negatively charged histidine–glutamate–histidine–glutamate–histidine–glutamate (HEHEHE)-tag permits purification of Affibody molecules by IMAC, enables labeling with [$^{99m}\text{Tc}(\text{CO})_3$]⁺, and provides low hepatic accumulation of radioactivity. In this study, we compared the biodistribution of cysteine-containing Affibody molecules site-specifically labeled with ^{111}In , ^{99m}Tc , and ^{125}I at the C-terminus, having a His₆-tag at the N- or C-terminus or a HEHEHE-tag at the N-terminus. We show that the use of a HEHEHE-tag provides appreciable reduction of hepatic radioactivity, especially for radiometal labels. We hope that this information can also be useful for development of other scaffold protein-based imaging agents.



INTRODUCTION

Radionuclide molecular imaging of tumor-associated molecular abnormalities has an appreciable potential to improve cancer treatment by stratifying patients for particular targeting therapy and by monitoring therapy response.^{1–3} A precondition for the clinical success of radionuclide molecular imaging is high specificity and sensitivity of the diagnostics, which depend on high accumulation of the radiolabeled imaging probe at the tumor sites and clearance of radioactivity from blood and healthy tissues. Scaffold proteins, such as Affibody molecules, knottins, and DARPins, have a great potential as imaging probes.⁴ Their small size (4–15 kDa) provides rapid extravasation and penetration of the extracellular space. It also provides rapid renal clearance of nonbound tracer. High affinity of the scaffold proteins for their target facilitates retention of radioactivity in the tumors. High tumor uptake and rapid clearance of nonbound radiolabeled scaffold proteins provide high imaging contrast, increasing the sensitivity of imaging. In addition, targeting proteins with molecular weight of less than 45 kDa such as the scaffold proteins mentioned above do not accumulate in tumors nonspecifically because of the “enhanced permeability and retention” (EPR) effect, further improving the specificity.⁵

Affibody molecules are derived from a modified version of the triple-helical B-domain of staphylococcal protein A.⁶ They are usually generated by phage display-based selection from libraries

where 13 surface-exposed amino acids in helices 1 and 2 have been randomized. Selections followed by affinity maturation have led to identification of Affibody binders to a variety of proteins⁷ with low nanomolar or even subnanomolar affinities. Several of these have been shown to be excellent probes providing high-contrast imaging of several tumor associated proteins in animal models.^{7,8} The Affibody scaffold is cysteine-free, and it is therefore possible to introduce a unique thiol functional group suitable for site-specific labeling by introduction of a single cysteine into the molecule. Bifunctional chelators or prosthetic groups including a thiol-reactive moiety can thereby be conveniently added to the Affibody molecules in a site-specific manner giving uniform conjugates with reproducible chemical and pharmacological properties.

Addition of a hexahistidine tag (His₆-tag) to the Affibody molecule confers several desirable features. First, it allows for convenient and efficient purification by immobilized metal ion affinity chromatography (IMAC).⁹ Second, it can be used for chelation of ^{99m}Tc -tricarbonyl ([$^{99m}\text{Tc}(\text{CO})_3$]⁺), providing stable and site-specific labeling.¹⁰ However, His₆-tag based labeling has been shown to increase the hepatic accumulation of radioactivity for Affibody molecules¹¹ as well as for other

Received: January 21, 2011

Published: April 28, 2011

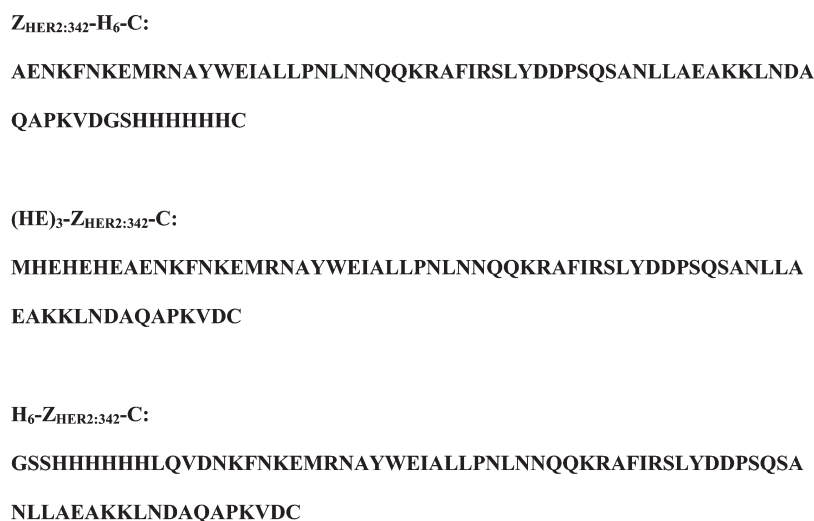


Figure 1. Sequences of the studied proteins.

imaging probes^{12–15} when evaluated *in vivo*. A high hepatic uptake is a very undesirable property of an imaging tracer, since the liver is a major metastatic site for many tumors. Our further studies showed that the His₆-tag itself was responsible for the elevated liver uptake at least for the Affibody molecules, since Affibody molecules, site-specifically labeled at the C-terminus with ^{99m}Tc using N₃S peptide-based cysteine-containing chelator or with ¹¹¹In using a maleimido derivative of DOTA, showed an increased liver uptake when compared to the same constructs without a His₆-tag.^{16,17}

Studies on the influence of labeling chemistry on biodistribution of Affibody molecules suggested that different chelators and labeling chemistries may influence their excretion pathway and hepatic uptake. More lipophilic and positively charged chelators at the N-terminus were associated with elevated hepatic uptake and/or hepatobiliary excretion of radioactivity.^{18,19} On the basis of these observations, we hypothesized that moving the His₆-tag to the C-terminus or replacing every second histidine with a negatively charged glutamate would reduce liver uptake of [^{99m}Tc(CO)₃]⁺-labeled Affibody molecules. To test the hypothesis, we compared variants of the anti-HER2 Affibody molecule Z_{HER2:342}, having a His₆-tag at the N- or C-terminus (designated H₆-Z_{HER2:342} of Z_{HER2:342}-H₆, respectively) or a histidine–glutamate–histidine–glutamate–histidine–glutamate (HEHEHE) tag at the N-terminus (designated as (HE)₃-Z_{HER2:342}). The results showed that moving the His₆-tag to the C-terminus or replacement of the His₆-tag with the HEHEHE-tag resulted in up to 10-fold lower hepatic accumulation of radioactivity with a similar tumor uptake for all three conjugates. This translated into appreciably superior tumor-to-liver ratio for [^{99m}Tc(CO)₃]⁺-labeled (HE)₃-Z_{HER2:342} compared to the alternative conjugates.²⁰

Improvement of the biodistribution of [^{99m}Tc(CO)₃]⁺-labeled Affibody molecules by using the HEHEHE-tag led us to hypothesize that the use of such a tag would be advantageous even if the Affibody molecule were designed to be labeled site-specifically at the C-terminus using different kinds of chemistries, since it would allow for convenient purification by IMAC. To verify this hypothesis, two new Affibody molecules were constructed, designated as Z_{HER2:342}-H₆-C and (HE)₃-Z_{HER2:342}-C. In the first construct, the hexahistidine tag was moved from the

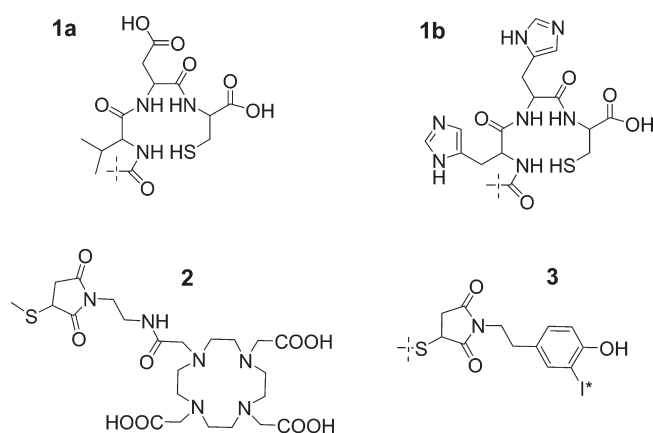


Figure 2. Chelators and linkers used for site-specific labeling of Affibody molecules. N₃S chelator for ^{99m}Tc: **1a**, VDC for (HE)₃-Z_{HER2:342}-C and H₆-Z_{HER2:342}-C; **1b**, HHC for Z_{HER2:342}-H₆-C. **2**: maleimido-monoamide-DOTA conjugated to C-terminal cysteine. **3**: iodo-HPEM conjugated to C-terminal cysteine.

N-terminus to the C-terminus. In the second construct, the hydrophilicity and negative charge of the N-terminal tag were increased by replacing three of the six histidine residues by glutamic acid residues, resulting in a HEHEHE-tag. To enable site-specific labeling, a cysteine was introduced at the C-terminus of each construct (Figure 1) which was addressed by several different labeling approaches (Figure 2). These constructs were compared head-to-head with the parental construct H₆-Z_{HER2:342}-C having a hexahistidine tag at the N-terminus and a cysteine at the C-terminus.

RESULTS

Production and Purification of Affibody Molecules. Affibody molecules were recombinantly produced in *Escherichia coli*. After harvest, disruption by sonication, and clarification, each lysate containing either the His₆-tagged Affibody molecule, Z_{HER2:342}-H₆-C, or the HEHEHE-tagged Affibody molecule, (HE)₃-Z_{HER2:342}-C, were heat-treated for 10 min at 60 °C to precipitate endogenous *E. coli* proteins prior to IMAC purification

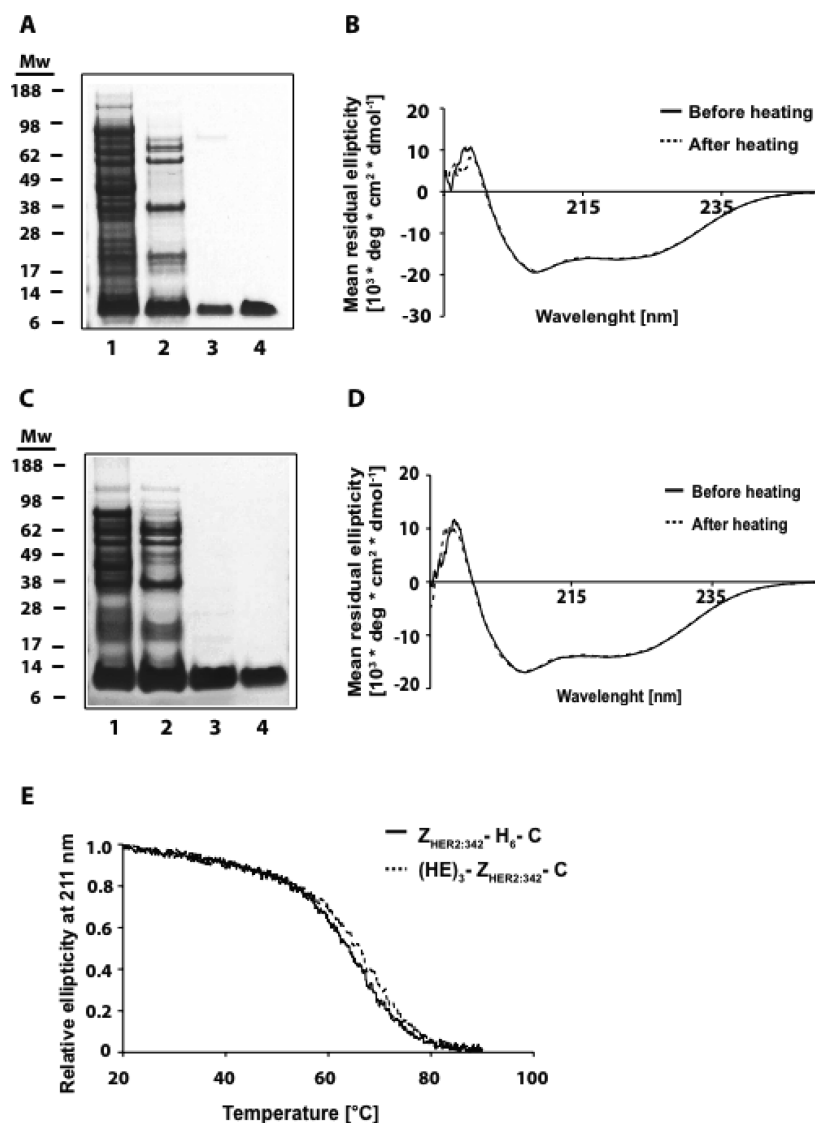


Figure 3. Analysis of $Z_{HER2:342}\text{-H}_6\text{-C}$ and $(HE)_3\text{-Z}_{HER2:342}\text{-C}$ Affibody molecules. SDS–PAGE analysis of samples taken during the purification of $Z_{HER2:342}\text{-H}_6\text{-C}$ (A) and $(HE)_3\text{-Z}_{HER2:342}\text{-C}$ (C): (lane 1) sample after cell lysis and initial clarification; (lane 2) sample after heat treatment; (lane 3) sample after IMAC purification; (lane 4) sample after RP-HPLC. (B) Overlay of CD spectrum recorded before and after thermal unfolding of $Z_{HER2:342}\text{-H}_6\text{-C}$. (D) Overlay of CD spectrum recorded before and after thermal unfolding of $(HE)_3\text{-Z}_{HER2:342}\text{-C}$. (E) Overlay of the ellipticity measured in a CD spectrometer at 221 nm as a function of temperature for $Z_{HER2:342}\text{-H}_6\text{-C}$ and $(HE)_3\text{-Z}_{HER2:342}\text{-C}$.

on a Co^{2+} derived affinity resin. Both $Z_{HER2:342}\text{-H}_6\text{-C}$ and $(HE)_3\text{-Z}_{HER2:342}\text{-C}$ could successfully be recovered by IMAC even though $(HE)_3\text{-Z}_{HER2:342}\text{-C}$ contained a reduced number of histidine residues in the purification tag. The Affibody molecules were further purified by reversed-phase high performance liquid chromatography (RP-HPLC) and analysis by sodium dodecyl sulfate–polyacrylamide gel electrophoresis (SDS–PAGE) of samples taken after IMAC and after RP-HPLC showed essentially pure proteins, with only a single band having a molecular weight corresponding to the expected molecular mass of the Affibody molecules (Figure 3).

Characterization of Affibody Constructs. Analyses of $Z_{HER2:342}\text{-H}_6\text{-C}$, $(HE)_3\text{-Z}_{HER2:342}\text{-C}$, and $\text{H}_6\text{-Z}_{HER2:342}\text{-C}$ by RP-HPLC showed a purity higher than 95% for each Affibody molecule (Table 1). Also, no obvious difference in RP-HPLC retention time between the three constructs was detected. Mass spectrometric analysis showed a good correlation of each Affibody molecule with their corresponding theoretical molecular mass (Table 1).

Table 1. Characteristics of the Affibody Molecules

	Affibody molecule		
	$(HE)_3\text{-Z}_{HER2:342}\text{-C}$	$Z_{HER2:342}\text{-H}_6\text{-C}$	$\text{H}_6\text{-Z}_{HER2:342}\text{-C}$
calculated M_w (Da)	7938	7975	8318
found M_w (Da)	7939	7976	8318
sample purity (%)	99.0	99.2	96
retention time (min)	16.4	16.0	16.4
T_m ($^{\circ}\text{C}$)	66	64	65
K_D (pM)	41	36	42
k_a ($\text{M}^{-1}\text{s}^{-1}$)	5.8×10^6	1.2×10^7	4.3×10^6
k_d (s^{-1})	2.4×10^{-4}	4.4×10^{-4}	1.8×10^{-4}

The dissociation equilibrium constant (K_D), the association rate constant (k_a), and the dissociation rate constant (k_d) for

Table 2. Labeling Yield and Radiochemical Purity of Affibody Molecules after Purification by Disposable NAP-5 Columns^a

	radiochemical yield, %	radiochemical purity, %
¹¹¹ In		
DOTA-(HE) ₃ -Z _{HER2:342} -C	98.9 ± 0.2	
DOTA-H ₆ -Z _{HER2:342} -C	99.2 ± 0.3	
DOTA-Z _{HER2:342} -H ₆ -C	99.4 ± 0.5	
¹²⁵ I		
(HE) ₃ -Z _{HER2:342} -C	32.0 ± 1.0	99.3 ± 0.2
H ₆ -Z _{HER2:342} -C	36.2 ± 3.0	99.1 ± 0.7
Z _{HER2:342} -H ₆ -C	36.0 ± 1.0	99.3 ± 0.4
^{99m} Tc		
(HE) ₃ -Z _{HER2:342} -C	76.5 ± 1.0	98.9 ± 0.3
H ₆ -Z _{HER2:342} -C	82.9 ± 2.0	99.7 ± 0.2
Z _{HER2:342} -H ₆ -C	99.3 ± 0.5	99.6 ± 0.1

^a Additional purification was not required for ¹¹¹In-labeled Affibody molecules. In all ^{99m}Tc-labeled conjugates, radiocolloid formation was less than 0.4%.

Z_{HER2:342}-H₆-C, (HE)₃-Z_{HER2:342}-C, and H₆-Z_{HER2:342}-C were determined by biosensor analysis. The *K_D* for H₆-Z_{HER2:342}-C was determined to be 42 pM, which correlates well with the previously determined 29 pM.¹⁶ Also, the *K_D* for Z_{HER2:342}-H₆-C and (HE)₃-Z_{HER2:342}-C was determined to be 36 and 41 pM, respectively (Table 1), indicating that the location and composition of the histidine-based tags have no apparent effect on the affinity between the Affibody molecule and HER2. Circular dichroism analyses showed that Z_{HER2:342}-H₆-C and (HE)₃-Z_{HER2:342}-C had melting temperatures of 64 and 66 °C (Table 1), respectively, which correlated well with the previously reported value of 65 °C for H₆-Z_{HER2:342}-C.¹⁶ As expected, all three Affibody molecules gave CD spectra showing high α -helical content (Figure 3). Also, the spectra recorded for each construct before and after heating from 20 to 90 °C were highly similar, indicating that all three constructs were able to completely refold after thermal denaturation (Figure 3).

Labeling of Conjugates. Site-specific labeling of (HE)₃-Z_{HER2:342}-C, Z_{HER2:342}-H₆-C, and H₆-Z_{HER2:342}-C with ^{99m}Tc, ¹²⁵I, and ¹¹¹In was performed according to methods developed earlier.^{16,21,22} ^{99m}Tc was attached using the N₃S chelator formed by the thiol from the C-terminal cysteine and amides from adjacent amino acids. ¹¹¹In was attached using maleimidomonoamide-DOTA (1,4,7,10-tetraazacyclododecane-1,4,7-tris-acetic acid 10-maleimidoethylacetamide), and ¹²⁵I was attached using HPEM (1-[2-(4-hydroxyphenyl)ethyl]pyrrole-2,5-dione) (Figure 2). Data concerning yield and radiochemical purity are presented in Table 2. Labeling of conjugates with ¹¹¹In provided high radiochemical purity (over 98%), and additional purification was not required. Simple purification of ¹²⁵I- and ^{99m}Tc-labeled Affibody molecules using disposable NAP-5 size-exclusion columns resulted in a radiochemical purity of more than 98%.

Binding Specificity of Radiolabeled Affibody Molecules to HER2-Expressing Cells in Vitro. Binding specificity tests (Table 3) indicated that the binding of all labeled Affibody constructs to living HER2-expressing cells was receptor mediated; saturation of the receptors by preincubation with nonlabeled Z_{HER2:342} significantly decreased the binding of the radiolabeled Affibody molecules.

Table 3. Specificity of Binding of Labeled Affibody Molecules to HER2-Expressing Cells in Vitro^a

	nonblocked	blocked
¹¹¹ In-DOTA-(HE) ₃ -Z _{HER2:342} -C	41.6 ± 3.2	1.0 ± 0.1
¹¹¹ In-DOTA-H ₆ -Z _{HER2:342} -C	51.3 ± 0.3	1.3 ± 0.2
¹¹¹ In-DOTA-Z _{HER2:342} -H ₆ -C	55.1 ± 0.4	1.2 ± 0.2
¹²⁵ I-HPEM-(HE) ₃ -Z _{HER2:342} -C	19.6 ± 1.0	8.9 ± 0.8
¹²⁵ I-HPEM-H ₆ -Z _{HER2:342} -C	25.7 ± 1.4	8.1 ± 0.5
¹²⁵ I-HPEM-Z _{HER2:342} -H ₆ -C	28.4 ± 0.5	8.0 ± 0.2
^{99m} Tc-(HE) ₃ -Z _{HER2:342} -C	23.8 ± 0.3	0.5 ± 0.0
^{99m} Tc-H ₆ -Z _{HER2:342} -C	44.5 ± 1.0	1.0 ± 0.2
^{99m} Tc-Z _{HER2:342} -H ₆ -C	21.2 ± 0.4	0.7 ± 0.1

^a The test was performed on the ovarian cancer cell line, SKOV-3. For presaturation of antigens, a 1000-fold molar excess of nonradioactive Affibody molecules was added. Data are presented as mean values of percent of added radioactivity that is cell-bound from three cell dishes and standard deviations. The difference between uptake by nonblocked and blocked cells was highly significant (*p* < 0.0005).

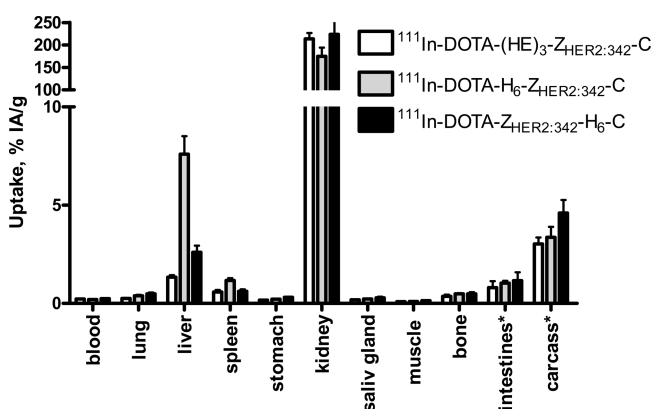


Figure 4. Biodistribution of ¹¹¹In-labeled Affibody molecules in female NMRI mice 4 h after intravenous injection. The concentration of radioactivity in different organs is expressed as % IA/g and presented as an average value from four animals ± standard deviation. (*) Data for intestines with content and carcass are presented as % of injected radioactivity per whole sample.

In Vivo Studies. Data on the comparative biodistribution of ¹¹¹In-DOTA-H₆-Z_{HER2:342}, ¹¹¹In-DOTA-Z_{HER2:342}-H₆-C, and ¹¹¹In-DOTA-(HE)₃-Z_{HER2:342}-C in female NMRI mice at 4 h after intravenous injection are presented in Figure 4. The general pattern of all three conjugates was typical for Affibody molecules, with a rapid clearance from blood and majority of organs and tissues. Low radioactivity in intestines (nonsignificant difference between conjugates) indicated low extent of hepatobiliary excretion of radioactivity. The renal clearance was apparently accompanied by reabsorption, which resulted in an appreciable accumulation of radioactivity in the kidneys (175–225 % IA/g at 4 h after injection). Within this pattern, appreciable differences in biodistribution of the conjugates with different tags were apparent. Tissue radioactivity concentration after injection of ¹¹¹In-DOTA-(HE)₃-Z_{HER2:342}-C was the lowest except from kidneys. ¹¹¹In-DOTA-H₆-Z_{HER2:342}-C had the highest uptake in liver and spleen. The liver uptake of ¹¹¹In-DOTA-H₆-Z_{HER2:342}-C was 5.7-fold higher than uptake of ¹¹¹In-DOTA-(HE)₃-Z_{HER2:342}-C and 2.8-fold higher than uptake of ¹¹¹In-DOTA-Z_{HER2:342}-H₆-C.

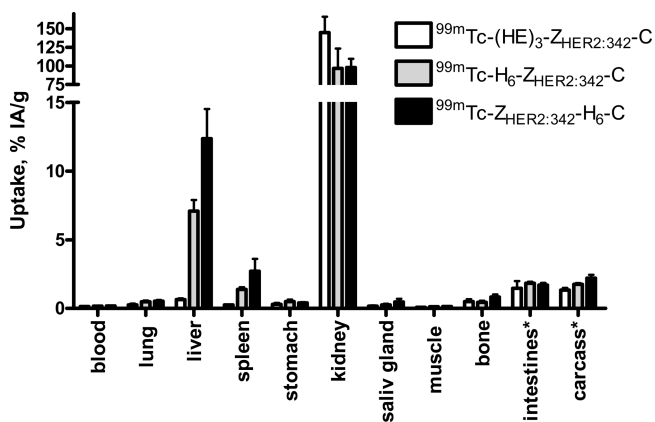


Figure 5. Biodistribution of ^{99m}Tc -labeled Affibody molecules in female NMRI mice 4 h after intravenous injection. The concentration of radioactivity in different organs is expressed as % IA/g and presented as an average value from four animals \pm standard deviation. (*) Data for intestines with content and carcass are presented as % of injected radioactivity per whole sample.

Accumulation of ^{111}In -DOTA- H_6 - $\text{Z}_{\text{HER2}:342}$ -C in the spleen was approximately 2-fold higher than the accumulation of other ^{111}In -labeled Affibody molecules. Pulmonary accumulation of both His₆-tag containing variants was significantly higher than the accumulation of ^{111}In -DOTA-(HE)₃- $\text{Z}_{\text{HER2}:342}$ -C.

Data on the comparative biodistribution of ^{99m}Tc -(HE)₃- $\text{Z}_{\text{HER2}:342}$ -C, ^{99m}Tc - H_6 - $\text{Z}_{\text{HER2}:342}$ -C, and ^{99m}Tc - $\text{Z}_{\text{HER2}:342}$ - H_6 -C in female NMRI mice at 4 h after intravenous injection are presented in Figure 5. The distribution of radioactivity for these conjugates is similar to the distribution observed for their ^{111}In -labeled counterparts, although renal retention of radioactivity was lower for ^{99m}Tc in comparison with ^{111}In . The low radioactivity level in intestines with content (less than 2% for all conjugates) suggested that the hepatobiliary pathway played a minor role in excretion of all conjugates. Accumulation of radioactivity in the stomach and salivary gland was low (less than 0.5% IA/g), indicating no release of ^{99m}Tc -pertechnetate during distribution of the conjugates or their catabolism. Similar to the ^{111}In -labeled constructs, the radioactivity accumulation in organs and tissues (except kidneys) was the lowest for the conjugate with the HEHEHE-tag. However, the influence of the histidine tag on hepatic uptake of ^{99m}Tc -labeled Affibody molecules was different from the uptake of the ^{111}In -labeled counterparts. The highest liver accumulation was observed for ^{99m}Tc - $\text{Z}_{\text{HER2}:342}$ - H_6 -C (12 ± 2 % IA/g), which was 19-fold higher than the liver accumulation of ^{99m}Tc -(HE)₃- $\text{Z}_{\text{HER2}:342}$ -C and 1.7-fold higher than accumulation of ^{99m}Tc - H_6 - $\text{Z}_{\text{HER2}:342}$ -C. Besides, the uptake of radioactivity in the spleen was appreciably higher for ^{99m}Tc - $\text{Z}_{\text{HER2}:342}$ - H_6 -C than for both other conjugates.

Biodistribution of radioiodinated Affibody molecules at 4 h after injection is presented in Figure 6. Similar to the ^{111}In and ^{99m}Tc labeled Affibody molecules, ^{125}I -HPEM- $\text{Z}_{\text{HER2}:342}$ - H_6 -C, ^{125}I -HPEM-(HE)₃- $\text{Z}_{\text{HER2}:342}$ -C, and ^{125}I -HPEM- H_6 - $\text{Z}_{\text{HER2}:342}$ -C demonstrated a rapid clearance from the blood. However, the use of nonresidualizing iodine resulted in a considerably lower level of renal retention of radioactivity than for the constructs containing residualizing radiometal labels (1.7–2.1 % IA/g). A higher radioactivity accumulation was instead observed in organs accumulating free iodide, i.e., the stomach and salivary gland, compared to the constructs labeled with ^{111}In or ^{99m}Tc .

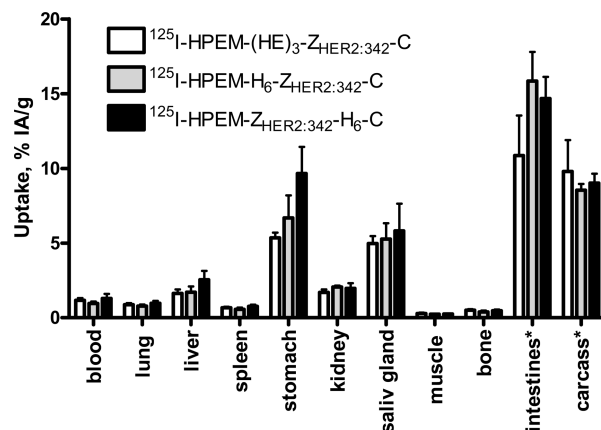


Figure 6. Biodistribution of ^{125}I -labeled Affibody molecules in female NMRI mice 4 h after intravenous injection. The concentration of radioactivity in different organs is expressed as % IA/g and presented as an average value from four animals \pm standard deviation. (*) Data for intestines with content and carcass are presented as % of injected radioactivity per whole sample.

Accumulation of radioactivity in the intestines with content (11–16% IA per whole sample) was appreciable, suggesting that hepatobiliary excretion of radioiodinated conjugates and/or their radiocatabolites plays a more substantial role for ^{125}I -labeled Affibody molecules than for the radiometal labeled counterparts. Accumulation of radioactivity in the liver after injection of ^{125}I -HPEM-(HE)₃- $\text{Z}_{\text{HER2}:342}$ -C (1.6 ± 0.3 % IA/g) was similar to the accumulation observed for ^{111}In -DOTA-(HE)₃- $\text{Z}_{\text{HER2}:342}$ -C (1.3 ± 0.1 % IA/g) but higher than for ^{99m}Tc -(HE)₃- $\text{Z}_{\text{HER2}:342}$ -C. Though the liver uptake of ^{125}I -HPEM- $\text{Z}_{\text{HER2}:342}$ - H_6 -C (2.3 ± 0.6 % IA/g) was significantly higher than the uptake of ^{125}I -HPEM-(HE)₃- $\text{Z}_{\text{HER2}:342}$ -C, the difference was less pronounced than the effect observed for the radiometal labels.

DISCUSSION AND CONCLUSION

Affibody molecules have demonstrated excellent results in high-contrast imaging of tumor-associated biomarkers both in preclinical studies⁸ and in a pilot clinical proof-of-principle study.²³ During development of the probes, numerous variants need to be evaluated, both in terms of amino acid composition of the actual Affibody molecule and in terms of composition of optimal chelators. Fitting the recombinantly produced variants with a His₆-tag allows simple purification by IMAC compared to more labor intensive purification schemes of the same constructs lacking a tag. However, fitting Affibody molecules with a His₆-tag leads to high liver accumulation,^{11,16,17} which is undesirable, since the liver is a major metastatic site of many tumors. The exact mechanism leading to elevated hepatic uptake of histidine containing proteins is unknown, as hepatocytes can take up peptides by several competing pathways.²⁴ Previous studies of radiolabeled Affibody molecules suggest that the overall lipophilicity of the conjugate, the local distribution of lipophilic and hydrophilic amino acids, and the presence of a positively charged N-terminal chelator can be associated with elevated hepatic uptake.^{20,25}

We have previously shown that the introduction of a HEHEHE-tag in the Affibody molecule allowed for IMAC purification using Ni^{2+} -loaded chelating sepharose and resulted in a reduced liver uptake compared to the same construct with a

His₆-tag where both constructs were specifically labeled on the histidine tag using [^{99m}Tc(CO)₃]⁺.²⁰ However, using a histidine-containing tags for labeling limits the radionuclides available for imaging agent design, which also limits the possibility of tailoring the imaging agent to fit a particular application. It is desirable to have a more general solution allowing attachment of different nuclides, associated with simple probe purification and favorable biodistribution.

This study was designed to evaluate if the use of a HEHEHE-tag provides improvements to the biodistribution compared to the use of a His₆-tag when site-specific labeling was performed at the C-terminus of the Affibody molecules using thiol-directed chemistry. In addition, the aim was to evaluate the influence of the His₆-tag positioning at the N- or C-terminus on biodistribution for different kinds of labels, since such information concerning structure–properties relationship provides input for design of future imaging probes.

Efficient IMAC purification was a precondition for successful application of the HEHEHE-tags. In our previous study²⁰ we used commercially available chelating Sepharose loaded with Ni²⁺ for purification of the HEHEHE-tagged Affibody molecules. The functional group on chelating Sepharose is iminodiacetic acid, a tridentate chelator that allows stronger binding of His-containing proteins than many other commercially available IMAC resins. We reasoned then that it could be necessary to use a resin with strong binding, since half of the histidines in the tag had been replaced with glutamate residues. In this work we investigated if the HEHEHE-tag also allowed purification by a resin that has a weaker interaction with His-containing proteins such as a Co²⁺-loaded Talon resin. We found that HEHEHE-tagged Affibody molecules were indeed able to interact with such a resin and the proteins could successfully be purified despite the substitution of three His-residues in the tag.

Importantly, all cysteine-containing variants retained a high affinity to HER2, independent of position and composition of the histidine-based tags (Table 1). The absence of negative influence of the HEHEHE-tag on the affinity of Z_{HER2:342} for the HER2 receptor has been shown for non-cysteine-containing counterparts.²⁰ Retained specificity of binding to HER2-expressing cells was demonstrated for all conjugates after labeling using all selected methods (Table 3). Earlier studies have demonstrated that Z_{HER2:342} derivatives, which had preserved specific *in vitro* binding to HER2-expressing cells after labeling, have been capable of HER2-specific accumulation in tumor xenografts. Saturation of HER2 in xenografts by preinjection of a large excess of nonlabeled Z_{HER2:342} was shown to provide significant reduction of tumor uptake of the labeled conjugates.^{11,16–20,25–28} The tumor uptake of non-HER2-specific Affibody molecules was 1–2% of the specific ones when labeled using the same methods.^{16,26}

In vivo biodistribution comparison was performed in this study at 4 h after injection, as previous studies have demonstrated that targeting of HER2-expressing xenografts using radiolabeled Z_{HER2:342} derivatives at this time point provides high tumor uptake (10–20 % IA/g for radiometals and over 9 % IA/g for radioiodine, depending on labeling chemistry) and high tumor-to-blood ratios (50–200 for radiometals and over 10 for radioiodine) in preclinical studies.^{16,17,22,27,28} A pilot clinical study has demonstrated that high contrast imaging of HER2-expressing metastases with ¹¹¹In-labeled DOTA-Z_{HER2:342} was possible at 4 h after injection.²³ This time point is consistent with clinical practice where tracer administration and image acquisition on the same day are preferred over protocols that extend over 2 or more days.

The results of this study confirmed the hypothesis that the HEHEHE-tag improves biodistribution of radiolabeled Affibody molecules in comparison to His₆-tag containing counterparts. The HEHEHE-tagged conjugates had the lowest hepatic uptake of all investigated constructs. The biggest advantages were observed for probes labeled with the residualizing radiometal labels, ¹¹¹In and ^{99m}Tc. For the nonresidualizing radioiodine label, the advantage in hepatic uptake was less evident. Uptake and internalization of proteins and peptides in the excretory organs (liver and kidneys) are associated with rapid proteolytic degradation. Lipophilic radiocatabolites of iodinated proteins “leak” through lysosomal and cellular membranes, leading to low intracellular retention of radiohalogen-associated radioactivity.^{11,29} In this case, ¹²⁵I-HPEM-(HE)₃-Z_{HER2:342}-C provided only 1.6-fold reduction of hepatic radioactivity in comparison with ¹²⁵I-HPEM-Z_{HER2:342}-H₆-C, and the difference between hepatic uptake of ¹²⁵I-HPEM-(HE)₃-Z_{HER2:342}-C and ¹²⁵I-HPEM-H₆-Z_{HER2:342}-C was not significant (Figure 6).

Catabolites of radiometals, such as ¹¹¹In and ^{99m}Tc, cannot easily penetrate lysosomal and cellular membranes and are efficiently retained intracellularly after proteolysis.²⁹ In this case, radioactivity concentration depends on an initial uptake and the advantage of the HEHEHE-tag over a His₆-tag was more evident (Figures 4 and 5).

For indium-111-labeled conjugates, the reduction of hepatic uptake of ¹¹¹In-DOTA-(HE)₃-Z_{HER2:342}-C was 5.7- and 2- fold, in comparison with ¹¹¹In-DOTA-H₆-Z_{HER2:342} and ¹¹¹In-DOTA-Z_{HER2:342}-H₆-C, respectively (Figure 4). The effect of position and composition of the histidine tag resembled the effect observed for the [^{99m}Tc(CO)₃]⁺ His-tag-directed label but was not as pronounced. It is noted that [^{99m}Tc(CO)₃]⁺ is quite lipophilic, while ¹¹¹In-DOTA is more hydrophilic, and the overall lipophilicity of ¹¹¹In-DOTA labeled conjugates is lower. Thus, the effect of a higher hydrophilicity of the HEHEHE-tag in comparison with the hexahistidine tag should not be as high for ¹¹¹In as for [^{99m}Tc(CO)₃]⁺. The liver uptake of ¹¹¹In-DOTA-(HE)₃-Z_{HER2:342}-C at 4 h pi (1.3 ± 0.1 % IA/g) was close to the hepatic uptake of the homologous ¹¹¹In-DOTA-Z_{HER2:2395}-C (1.5 ± 0.3 % IA/g) Affibody molecule,²⁷ which was labeled using the same chelator but did not contain any histidine tag.

The liver uptake of ^{99m}Tc-(HE)₃-Z_{HER2:342}-C at 4 h after injection (0.65 ± 0.09 % IA/g) was appreciably reduced in comparison with the uptake of ^{99m}Tc-H₆-Z_{HER2:342}-C (7.1 ± 0.8 % IA/g) and ^{99m}Tc-Z_{HER2:342}-H₆-C (12.0 ± 2 % IA/g) (Figure 5). Interestingly, it was also lower than the uptake of the homologous non-His-tag-containing ^{99m}Tc-Z_{HER2:2395}-C, which has been earlier site-specifically labeled using the same cysteine-containing peptide-based N₃S chelator (VDC) at the C-terminus (1.2 ± 0.2 % IA/g).¹⁷ Thus, the use of a HEHEHE-tag provides a lower hepatic uptake in combination with a ^{99m}Tc-N₃S-labeling chemistry not only in comparison with His₆-tag-containing probes, irrespective of tag position, but also in comparison with a homologous conjugate, which does not contain any histidine tag. This suggests that the HEHEHE-tag might be used in the future for improving biodistribution of imaging agents.

An interesting phenomenon is an elevated hepatic uptake of ^{99m}Tc-Z_{HER2:342}-H₆-C in comparison with ^{99m}Tc-H₆-Z_{HER2:342}-C because it contradicts the tendency seen with other labels. It should be noted that in the case of ^{99m}Tc-labeled Affibody molecules, the labeling chemistry is not the same for all three conjugates.

The N_3S chelator for the $[^{99m}\text{Tc}(\text{V})\text{O}]^{3+}$ core is VDC in the case of $^{99m}\text{Tc}-(\text{HE})_3\text{-Z}_{\text{HER2:342}}\text{-C}$ and $^{99m}\text{Tc}\text{-H}_6\text{-Z}_{\text{HER2:342}}\text{-C}$ and is HHC in the case of $^{99m}\text{Tc}\text{-Z}_{\text{HER2:342}}\text{-H}_6\text{-C}$. We have found earlier that amino acid composition of the N_3S chelator can appreciably influence biodistribution and excretion pathway of ^{99m}Tc -labeled Affibody molecules.^{18,19,25,28} Thus, while the difference in liver uptake of $^{99m}\text{Tc}-(\text{HE})_3\text{-Z}_{\text{HER2:342}}\text{-C}$ and $^{99m}\text{Tc}\text{-H}_6\text{-Z}_{\text{HER2:342}}\text{-C}$ should be attributed to the influence of histidine tag composition, the high liver uptake of $^{99m}\text{Tc}\text{-Z}_{\text{HER2:342}}\text{-H}_6\text{-C}$ can also be due to the influence of the radiometal chelate. This effect deserves further investigations but is out of the scope of the current study.

This study was concentrated on the reduction of radioactivity uptake of imaging agents in the liver. The issue of renal uptake and retention of radioactivity after injection of Affibody molecules is out of the scope of this study but deserves a brief discussion. High renal radioactivity accumulation can be a serious problem for radionuclide therapy. However, this problem is not as severe for imaging applications because the dose to the kidneys would be much lower than in therapy. In addition, renal metastases are infrequent.^{30,31} Although high activity in the kidneys can obscure tumor uptake in the immediate area, an elevated renal uptake is considered to be more acceptable than high hepatobiliary excretion and the renal elimination route is desirable for imaging tracers.³² Renal uptake might be reduced by optimizing labeling chemistry. The results of this and other studies²⁹ suggest that the use of nonresidualizing radiohalogen labels is one way to decrease renal retention of radionuclides after injection of Affibody molecules. Our recent findings has demonstrated that optimization of the amino acid composition of a peptide-based cysteine-containing chelator can reduce renal retention of ^{99m}Tc dramatically.^{25,28}

The labeling methods evaluated in the current study were selected to represent some of the most common approaches to labeling. The C-terminal cysteine, together with amide nitrogens of the nearest amino acids, forms a N_3S chelator that can be used for labeling of proteins and peptides with ^{99m}Tc ^{17,33,34} and ^{186/188}Re.³⁵ Thus, Affibody molecules labeled in this way can be used for imaging with ^{99m}Tc , and it is possible that they may also be suitable for therapy with rhenium isotopes. The use of a maleimido derivative of DOTA provides stable labeling with nuclides such as ¹¹¹In for SPECT or ⁶⁸Ga, ⁸⁶Y, and ⁵⁵Co for PET. Our experiments have previously shown that the general biodistribution pattern of Affibody molecules would be very similar, although not identical, for different DOTA-chelated radiometals.^{36,37} Furthermore, ¹²⁵I was used in this study as a surrogate for ¹²³I ($T_{1/2} = 13.3$ h), which is a suitable nuclide for SPECT. However, the biodistribution of Affibody molecules labeled with radioiodine using HPEM²² is very similar to the biodistribution of Affibody molecules labeled for PET with ⁷⁶Br using HPEM³⁸ or with ¹⁸F using FBEM.³⁹ Thus, the results of the current study can be, hopefully, reliably projected to biodistribution of Affibody molecules labeled with other radionuclides.

In conclusion, the use of the HEHEHE-tag permits efficient and simple purification of Affibody molecules. This tag has no negative effect on the affinity of the Affibody molecules to its molecular target. The HEHEHE-containing Affibody molecules also retained specific binding to HER2-expressing cells after labeling with several nuclides using different labeling chemistries. The use of the HEHEHE-tags improved biodistribution (reduced hepatic uptake) of radiolabeled Affibody molecules when several different approaches to labeling were investigated.

We suggest that HEHEHE-tags should be used in the future for purification of Affibody molecules irrespective of what labeling chemistry is considered. We also hope that the use of HEHEHE-tags would be advantageous for other targeting probes derived from scaffold proteins for in vivo radionuclide imaging.

EXPERIMENTAL SECTION

General. High-quality Milli-Q water (resistance higher than 18 M Ω /cm) was used for preparing solutions. Maleimidomonoamide-DOTA was purchased from Macrocyclics (Dallas, TX, U.S.). ((4-Hydroxyphenyl)ethyl)maleimide (HPEM) has been synthesized and characterized in our laboratories, as described by earlier.³⁸ [¹¹¹In]Indium chloride was purchased from Covidien. Sodium [¹²⁵I]iodide was from Perkin-Elmer. ^{99m}Tc was obtained as pertechnetate from an Ultra-TechneKow generator (Covidien) by elution with sterile 0.9% NaCl. NAP-5 size exclusion columns were from GE Healthcare, Uppsala, Sweden. Buffers, 0.1 M phosphate buffered saline (PBS), pH 7.5, and 0.2 M ammonium acetate, were prepared using common methods from chemicals supplied by Merck (Darmstadt, Germany). Buffers, which were used for conjugation with DOTA and labeling with ¹¹¹In, were purified from metal contamination using Chelex 100 resin (Bio-Rad Laboratories, Richmond, CA, U.S.). Cells used during in vitro experiments were detached using trypsin–EDTA solution (0.25% trypsin, 0.02% EDTA in buffer, Biochrom AG, Berlin, Germany). For in vivo experiments Ketalar (50 mg/mL, Pfizer, NY, U.S.), Rompun (20 mg/mL, Bayer, Leverkusen, Germany), and heparin (5000 IE/mL, Leo Pharma, Copenhagen, Denmark) were used. Data on cellular uptake and biodistribution were assessed by an unpaired two-tailed *t*-test using GraphPad Prism (version 4.00 for Windows GraphPad Software, San Diego, CA, U.S.) in order to determine any significant differences ($p < 0.05$). Radioactivity was measured using an automated γ -counter with a 3-in. NaI(Tl) detector (1480 WIZARD, Wallac Oy, Turku, Finland). The distribution of radioactivity along the thin layer chromatography strips and SDS–PAGE gels was measured on a Cyclone storage phosphor system and analyzed using the OptiQuant image analysis software (PerkinElmer).

Production, Purification, and Characterization of $Z_{\text{HER2:342}}\text{-H}_6\text{-C}$ and $(\text{HE})_3\text{-Z}_{\text{HER2:342}}\text{-C}$ Affibody Molecules. The production and purification of Affibody molecules $Z_{\text{HER2:342}}\text{-H}_6\text{-C}$ and $(\text{HE})_3\text{-Z}_{\text{HER2:342}}\text{-C}$ were essentially done as previously described.²⁰ Briefly, PCR fragments encoding $Z_{\text{HER2:342}}\text{-H}_6\text{-C}$ and $(\text{HE})_3\text{-Z}_{\text{HER2:342}}\text{-C}$ were subcloned into the expression vector pET21a(+) (Novagen, Darmstadt, Germany) and correct DNA sequences were verified by DNA sequencing. Affibody molecules were expressed in *Escherichia coli* strain BL21(DE3) as previously described.⁴⁰ After cell disruption by sonication followed by cell debris removal by centrifugation, the clarified cell lysates were heat-treated for 10 min at 60 °C. $Z_{\text{HER2:342}}\text{-H}_6\text{-C}$ and $(\text{HE})_3\text{-Z}_{\text{HER2:342}}\text{-C}$ were recovered by IMAC using a Talon metal affinity resin (BD Bioscience, San Jose, CA). The $\text{H}_6\text{-Z}_{\text{HER2:342}}\text{-C}$ Affibody molecule was kindly provided by Affibody AB, Stockholm, Sweden.

$Z_{\text{HER2:342}}\text{-H}_6\text{-C}$ and $(\text{HE})_3\text{-Z}_{\text{HER2:342}}\text{-C}$ were further purified by reverse phase high-performance liquid chromatography (RP-HPLC) on an Agilent 1200 HPLC system (Agilent Technologies, Santa Clara, CA). To reduce potential disulfide bridges, TCEP-HCl (Sigma-Aldrich, Sweden) was added to a final concentration of 50 mM followed by incubation at room temperature for 1 h prior to RP-HPLC purification. Samples were injected onto a C18 column using a 20 min gradient of 20–65% B (A, 0.1% TFA–H₂O; B, 0.1% TFA–CH₃CN), with a flow rate of 1.5 mL/min. The final purity of $Z_{\text{HER2:342}}\text{-H}_6\text{-C}$, $(\text{HE})_3\text{-Z}_{\text{HER2:342}}\text{-C}$, and $\text{H}_6\text{-Z}_{\text{HER2:342}}\text{-C}$ samples was analyzed by analytic RP-HPLC as previously described.²⁰ The purity was determined by dividing the area of the peak corresponding to the Affibody molecule with the total area of all peaks in

the chromatogram. Protein concentrations were determined by amino acid analysis (Amino Acid Analysis Center, Uppsala University).

Mass Spectrometry Analysis. The molecular masses of $Z_{\text{HER2:342}}\text{-H}_6\text{-C}$, $(\text{HE})_3\text{-Z}_{\text{HER2:342}}\text{-C}$, and $\text{H}_6\text{-Z}_{\text{HER2:342}}\text{-C}$ were determined on a 6520 Accurate-Mass Q-TOF LC/MS instrument (Agilent Technologies, Santa Clara, CA), and the isotopic and charge state information was deconvoluted using Agilent MassHunter B.02.00 software (Agilent Technologies).

Melting Point Analysis. Variable temperature measurements of $Z_{\text{HER2:342}}\text{-H}_6\text{-C}$, $(\text{HE})_3\text{-Z}_{\text{HER2:342}}\text{-C}$, and $\text{H}_6\text{-Z}_{\text{HER2:342}}\text{-C}$ were performed using a JASCO J-810 spectropolarimeter instrument (JASCO, Tokyo, Japan). Samples were diluted to 60 μM in PBS, and absorbance was measured at 221 nm using a temperature gradient increasing 5 $^\circ\text{C}/\text{min}$ and ranging from 20 to 90 $^\circ\text{C}$. Circular dichroism spectra were also recorded from 250 to 195 nm at 20 $^\circ\text{C}$ before and after each variable temperature measurement.

Biosensor Analysis. Real-time biospecific interaction analyses on a Biacore 3000 instrument (Biacore Life Science, GE Healthcare, Uppsala, Sweden) were performed to determine the affinity between HER-2 and $Z_{\text{HER2:342}}\text{-H}_6\text{-C}$, $(\text{HE})_3\text{-Z}_{\text{HER2:342}}\text{-C}$, and $\text{H}_6\text{-Z}_{\text{HER2:342}}\text{-C}$, respectively. Prior to analysis, the Affibody molecules were reduced with 30 mM DTT (dithiothreitol) followed by cysteine alkylation in the presence of 5 \times molar excess of *N*-ethylmaleimide. Recombinant human HER2-ECD fused to the Fc region of human IgG (R&D Systems, Minneapolis, MN) was immobilized (~ 2000 RU) on a flow-cell surface of a CMS sensor chip (Biacore Life Science, GE Healthcare, Uppsala, Sweden) by amine coupling, according to the manufacturer's instructions.

A 3-fold dilution series consisting of five different concentrations were prepared in duplicate for each Affibody construct. Samples were injected with a flow rate of 50 $\mu\text{L}/\text{min}$, and regeneration of the flow-cell surface was accomplished by injecting 20 μL of 15 mM HCl. The concentrations used were 50 pM to 3.8 nM for $Z_{\text{HER2:342}}\text{-H}_6\text{-C}$, 160 pM to 13 nM for $(\text{HE})_3\text{-Z}_{\text{HER2:342}}\text{-C}$, and 60 pM to 4.5 nM for $\text{H}_6\text{-Z}_{\text{HER2:342}}\text{-C}$. Finally, the dissociation equilibrium constant (K_D), the association rate constant (k_a), and the dissociation rate constant (k_d) were calculated using BIAevaluation 3.2 software (Biacore Life Science, GE Healthcare, Uppsala, Sweden), assuming a one-to-one interaction model.

Radiolabeling of Affibody Molecules. ^{111}In . Site-specific labeling of Affibody molecules with ^{111}In was performed according to the method described earlier.¹⁶ Briefly, spontaneously formed disulfide bonds in cysteine-containing Affibody molecules (0.125 μmol) were reduced by treatment with 30 mM dithiothreitol (DTT) (E. Merck, Darmstadt, Germany) in PBS during 2 h at 40 $^\circ\text{C}$. After reduction, the Affibody molecules were purified from DTT using a disposable NAP-5 size-exclusion column, pre-equilibrated and eluted with degassed 0.2 M ammonium acetate, pH 6.4. The Affibody molecules were mixed with double molar excess of maleimidomonoamide-DOTA (1 mg/mL in degassed 0.2 M ammonium acetate, pH 6.4). The vials were filled with argon gas and incubated at 38 $^\circ\text{C}$ overnight. The conjugates were purified from unconjugated chelator using a NAP-5 size-exclusion column, pre-equilibrated and eluted with 0.2 M ammonium acetate, pH 5.5. Aliquots containing 50 μg of DOTA-conjugated Affibody molecules in 90 μL of 0.2 M ammonium acetate, pH 5.5, have been prepared and stored frozen at -20 $^\circ\text{C}$.

For labeling, an aliquot was thawed, mixed with 30 μL (20–25 MBq) [^{111}In]indium chloride, and incubated at 60 $^\circ\text{C}$ for 40 min. Analysis was performed using 150-771 DARK GREEN Tec-Control Chromatography strips from Biodex Medical Systems (New York, U.S.) eluted with 0.2 M citric acid, pH 2.0. In this system, radiolabeled Affibody molecules remain at the application point and free ^{111}In migrates with the solvent front. The method has been cross-validated by SDS-PAGE. Since the radiochemical purity of the ^{111}In -labeled Affibody molecules was higher than 98%, no further purification was performed. Radiolabeled conjugates were diluted with PBS for biological experiments.

¹²⁵I. Radioiodination using HPEM was performed according to the method developed and validated earlier.²² Before radioiodination, spontaneously formed disulfide bridges between the Affibody molecules were reduced by incubation with DTT, as described above. The reduced Affibody molecules were used for labeling within 10–15 min after reduction. The amount of reduced Affibody molecules was determined and mixed with an equimolar amount with HPEM (typically 33 nmol).

For a radioiodination of HPEM, an amount of 15 μL of [^{125}I]iodide stock solution (30 MBq) was mixed with 15 μL of 5% solution of acetic acid in methanol and with 10 μL of solution of HPEM (46 nmol, 1 mg/mL in 5% solution of acetic acid in methanol). Chloramine-T (10 μL , 1.5 mg/mL in 5% solution of acetic acid in methanol) was added. The mixture was vortexed and then incubated for 5 min at ambient temperature. The reaction was quenched by adding 10 μL of sodium metabisulfite (3 mg/mL in water). Immediately after labeling of HPEM, an equimolar amount of Affibody molecule (solution in 0.2 acetate buffer, pH 6.4) was added, and the mixture was incubated at room temperature for 30 min. The yield was determined by 150-771 DARK GREEN Tec-Control Chromatography strips eluted with 70% acetone in water. Radiolabeled Affibody molecules remain at the application point, while iodide and I-HPEM migrate with the solvent front. The radiolabeled conjugate was purified using NAP-5 columns pre-equilibrated with PBS. The radiochemical purity of the conjugates was assessed using 150-771 DARK GREEN strips eluted with 70% acetone in water.

^{99m}Tc. Labeling of Affibody molecules with ^{99m}Tc was performed using a two-vial kit as described earlier.²¹ Briefly, labeling kits, containing 5 mg of sodium α -D-gluconate (Sigma-Aldrich, Steinheim, German), 100 μg of disodium edentate (Sigma-Aldrich, Steinheim, German), and 75 μg of tin(II) chloride dihydrate (Fluka Chemika, Buchs, Switzerland) each, were prepared and freeze-dried. For labeling, a kit was reconstituted in 100 μL of PBS and added to a vial containing 100 μg (12.5 nmol) of Affibody molecule. An amount of 100 μL of generator eluate (400–500 MBq) was added. The mixture was vortexed, and the vial was filled with argon gas, sealed, and incubated at 90 $^\circ\text{C}$ for 60 min. Thereafter, 1 μL samples were taken for analysis of the labeling yield using 150-771 DARK GREEN strips eluted with PBS and of reduced hydrolyzed technetium colloid (RHT) levels using 150-771 DARK GREEN strips eluted pyridine/acetic acid/water (10:6:3) as the mobile phase. The radiolabeled conjugates were purified using NAP-5 columns pre-equilibrated with PBS. The radiochemical purity of the conjugates was assessed using 150-771 DARK GREEN strips eluted with PBS.

Binding Specificity of Radiolabeled Affibody Molecules to HER2-Expressing Cells in Vitro. Specificity of binding of radiolabeled Affibody molecules to HER2-expressing cells in vitro was evaluated by the method described earlier.²⁰ The SKOV-3 ovarian carcinoma cell line (purchased from American Type Tissue Culture Collection (ATCC) via LGC Promochem, Borås, Sweden) was used. Labeled conjugates at 0.5 nM were added to the cell dishes. To one set of dishes, nonlabeled $Z_{\text{HER2:342}}$ at 0.5 μM was added 0.5 h before the labeled conjugate to saturate receptors on cells. The total volume in each well was 1 mL. Each experiment was done in triplicate. Cells were incubated for 1 h at 37 $^\circ\text{C}$. Thereafter the medium was collected and cells were washed once with cold serum-free medium and detached by treatment with 0.5 mL of trypsin-EDTA for 10–15 min at 37 $^\circ\text{C}$. Complete medium (0.5 mL) was added to the cells. The Cells were resuspended and cell suspension was collected and measured together with the corresponding incubation media for radioactivity content. The percent of cell-bound radioactivity was determined for each set of cell samples.

In Vivo Studies. All animal experiments were planned and performed in accordance with national legislation on laboratory animals' protection and were approved by the Local Ethics Committee for Animal Research.

Female NMRI mice (18 weeks old, weight 24–29 g) were used in the biodistribution studies. A group of four mice was used for each data

point. The animals were intravenously injected with 5 μ g of radiolabeled conjugate diluted in 100 μ L of PBS. The injected radioactivity was 40 kBq. The mice were euthanized at 4 h after injection by an intraperitoneal injection of Ketalar–Rompun solution (20 μ L of solution per gram of body weight: Ketalar, 10 mg/mL; Rompun, 1 mg/mL) followed by heart puncture with a 1 mL syringe rinsed with Heparine (5000 IE/mL). Blood and organ samples (lung, liver, spleen, stomach, kidneys, salivary gland, muscle, bone, intestines (with content)) and the remaining carcass were collected and weighed, and their radioactivity was measured. The organ uptake values are expressed as percent of injected activity per gram of tissue (% IA/g) except for the intestines and the remaining carcass, where values are expressed as % IA per whole sample.

AUTHOR INFORMATION

Corresponding Author

*Phone: +46 18 471 3414. Fax: + 46 18 471 3432. E-mail: vladimir.tolmachev@bms.uu.se.

ACKNOWLEDGMENT

This research was financially supported by grants from Swedish Cancer Society (Cancerfonden), Swedish Research Council (Vetenskapsrådet), and the O.E and Edla Johanssons foundation.

ABBREVIATIONS USED

IMAC, immobilized metal ion affinity chromatography; His₆, hexahistidine; HEHEHE, charged histidine–glutamate–histidine–glutamate–histidine–glutamate; DARPIn, designed ankyrin repeat proteins; EPR, enhanced permeability and retention; DOTA, 1,4,7,10-tetraazacyclododecane-1,4,7,10-tetraacetic acid; RP-HPLC, reversed-phase high performance liquid chromatography; SDS–PAGE, sodium dodecyl sulfate–polyacrylamide gel electrophoresis; K_D , dissociation equilibrium constant; k_a , the association rate constant; k_d , dissociation rate constant; HPEM, 1-[2-(4-hydroxyphenyl)ethyl]pyrrole-2,5-dione; SPECT, single photon emission computed tomography; PET, positron emission tomography; FBEM, N-[2-(4-[¹⁸F]fluorobenzamido)-ethyl]maleimido; Q-TOF LC/MS, quadrupole time-of-flight liquid chromatography–mass spectrometry; DTT, dithiothreitol; ECD, extracellular domain; EDTA, ethylenediaminetetraacetic acid

REFERENCES

- (1) Kelloff, G. J.; Krohn, K. A.; Larson, S. M.; Weissleder, R.; Mankoff, D. A.; Hoffman, J. M.; Link, J. M.; Guyton, K. Z.; Eckelman, W. C.; Scher, H. I.; O'Shaughnessy, J.; Cheson, B. D.; Sigman, C. C.; Tatum, J. L.; Mills, G. Q.; Sullivan, D. C.; Woodcock, J. The progress and promise of molecular imaging probes in oncologic drug development. *Clin. Cancer Res.* **2005**, *11*, 7967–7985.
- (2) McLarty, K.; Reilly, R. M. Molecular imaging as a tool for personalized and targeted anticancer therapy. *Clin. Pharmacol. Ther.* **2007**, *81*, 420–424.
- (3) Tolmachev, V.; Stone-Elender, S.; Orlova, A. Radiolabelled receptor-tyrosine-kinase targeting drugs for patient stratification and monitoring of therapy response: prospects and pitfalls. *Lancet Oncol.* **2010**, *11*, 992–1000.
- (4) Miao, Z.; Levi, J.; Cheng, Z. Protein scaffold-based molecular probes for cancer molecular imaging. *Amino Acids* [Online early access]. DOI: 10.1007/s00726-010-0503-9. Published Online: Feb 21, 2010.

- (5) Wester, H. J.; Kessler, H. Molecular targeting with peptides or peptide–polymer conjugates: just a question of size? *J. Nucl. Med.* **2005**, *46*, 1940–1945.
- (6) Nygren, P. A. Alternative binding proteins: affibody binding proteins developed from a small three-helix bundle scaffold. *FEBS J.* **2008**, *275*, 2668–2676.
- (7) Löfblom, J.; Feldwisch, J.; Tolmachev, V.; Carlsson, J.; Ståhl, S.; Frejd, F. Y. Affibody molecules: engineered proteins for therapeutic, diagnostic and biotechnological applications. *FEBS Lett.* **2010**, *584*, 2670–2680.
- (8) Ahlgren, S.; Tolmachev, V. Radionuclide molecular imaging using Affibody molecules. *Curr. Pharm. Biotechnol.* **2010**, *11*, 581–589.
- (9) Block, H.; Maertens, B.; Priestestersbach, A.; Brinker, N.; Kubicek, J.; Fabis, R.; Labahn, J.; Schäfer, F. Immobilized-metal affinity chromatography (IMAC): a review. *Methods Enzymol.* **2009**, *463*, 439–473.
- (10) Waibel, R.; Alberto, R.; Willuda, J.; Finnern, R.; Schibli, R.; Stichelberger, A.; Egli, A.; Abram, U.; Mach, J. P.; Plüchthun, A.; Schubiger, P. A. Stable one-step technetium-99m labeling of His-tagged recombinant proteins with a novel Tc(I)-carbonyl complex. *Nat. Biotechnol.* **1999**, *17*, 897–901.
- (11) Orlova, A.; Nilsson, F. Y.; Wikman, M.; Widström, C.; Ståhl, S.; Carlsson, J.; Tolmachev, V. Comparative in vivo evaluation of technetium and iodine labels on an anti-HER2 affibody for single-photon imaging of HER2 expression in tumors. *J. Nucl. Med.* **2006**, *47*, 512–519.
- (12) Berndorff, D.; Borkowski, S.; Moosmayer, D.; Viti, F.; Müller-Tiemann, B.; Sieger, S.; Friebe, M.; Hilger, C. S.; Zardi, L.; Neri, D.; Dinkelborg, L. M. Imaging of tumor angiogenesis using ^{99m}Tc-labeled human recombinant anti-ED-B fibronectin antibody fragments. *J. Nucl. Med.* **2006**, *47*, 1707–1716.
- (13) Zahnd, C.; Kawe, M.; Stumpp, M. T.; de Pasquale, C.; Tamaskovic, R.; Nagy-Davidescu, G.; Dreier, B.; Schibli, R.; Binz, H. K.; Waibel, R.; Plüchthun, A. Efficient tumor targeting with high-affinity designed ankyrin repeat proteins: effects of affinity and molecular size. *Cancer Res.* **2010**, *70*, 1595–1605.
- (14) Pimentel, G. J.; Vazquez, J. E.; Quesada, W.; Felipe, Y.; Carderón, C.; Freyre, F. M.; Oliva, J. P.; Gaviñondo, J. V. Hexa-histidine tag as a novel alternative for one-step direct labelling of a single-chain Fv antibody fragment with ^{99m}Tc. *Nucl. Med. Commun.* **2001**, *22*, 1089–1094.
- (15) Francis, R. J.; Mather, S. J.; Chester, K.; Sharma, S. K.; Bhatia, J.; Pedley, R. B.; Waibel, R.; Green, A. J.; Begent, R. H. Radiolabelling of glycosylated MFE-23::CPG2 fusion protein (MFECP1) with ^{99m}Tc for quantitation of tumour antibody-enzyme localisation in antibody-directed enzyme pro-drug therapy (ADEPT). *Eur. J. Nucl. Med. Mol. Imaging* **2004**, *31*, 1090–1096.
- (16) Ahlgren, S.; Orlova, A.; Rosik, D.; Sandström, M.; Sjöberg, A.; Bastrup, B.; Widmark, O.; Fant, G.; Feldwisch, J.; Tolmachev, V. Evaluation of maleimide derivative of DOTA for site-specific labeling of recombinant Affibody molecules. *Bioconjugate Chem.* **2008**, *19*, 235–243.
- (17) Ahlgren, S.; Wällberg, H.; Tran, T. A.; Widström, C.; Hjertman, M.; Abrahmsén, L.; Berndorff, D.; Dinkelborg, L. M.; Cyr, J. E.; Feldwisch, J.; Orlova, A.; Tolmachev, V. Targeting of HER2-expressing tumors using a site-specifically ^{99m}Tc-labeled recombinant Affibody molecule Z_{HER2.2.395} with C-terminal engineered cysteine. *J. Nucl. Med.* **2009**, *50*, 781–789.
- (18) Tran, T.; Engfeldt, T.; Orlova, A.; Sandström, M.; Feldwisch, J.; Abrahmsén, L.; Wennborg, A.; Tolmachev, V.; Karlström, A. E. ^{99m}Tc-maEEE-Z_{HER2.342}, an Affibody molecule-based tracer for the detection of HER2 expression in malignant tumors. *Bioconjugate Chem.* **2007**, *18*, 1956–1964.
- (19) Tran, T.; Ekblad, T.; Orlova, A.; Widström, C.; Feldwisch, J.; Wennborg, A.; Abrahmsén, L.; Tolmachev, V.; Eriksson Karlström, A. Effects of lysine-containing mercaptoacetyl-based chelators on the biodistribution of ^{99m}Tc-labeled anti-HER2. *Bioconjugate Chem.* **2008**, *19*, 2568–2576.
- (20) Tolmachev, V.; Hofström, C.; Malmberg, J.; Ahlgren, S.; Hosseinimehr, S. J.; Sandström, M.; Abrahmsén, L.; Orlova, A.

Gräslund, T. HEHEHE-tagged Affibody molecules may be purified by IMAC, are conveniently labeled with $[^{99m}\text{Tc}(\text{CO})_3]^+$, and show improved biodistribution. *Bioconjugate Chem.* **2010**, *21*, 2013–2022.

(21) Ahlgren, S.; Andersson, K.; Tolmachev, V. Kit formulation for ^{99m}Tc -labeling of recombinant anti-HER2 Affibody molecules with a C-terminally engineered cysteine. *Nucl. Med. Biol.* **2010**, *37*, 539–546.

(22) Tolmachev, V.; Mume, E.; Sjöberg, S.; Frejd, F. Y.; Orlova, A. Influence of valency and labelling chemistry on in vivo targeting using radioiodinated HER2-binding Affibody molecules. *Eur. J. Nucl. Med. Mol. Imaging* **2009**, *36*, 692–701.

(23) Baum, R. P.; Prasad, V.; Müller, D.; Schuchardt, C.; Orlova, A.; Wennborg, A.; Tolmachev, V.; Feldwisch, J. Molecular imaging of HER2-expressing malignant tumors in breast cancer patients using synthetic ^{111}In - or ^{68}Ga -labeled affibody molecules. *J. Nucl. Med.* **2010**, *51*, 892–897.

(24) Klaassen, C. D.; Aleksunes, L. M. Xenobiotic, bile acid, and cholesterol transporters: function and regulation. *Pharmacol. Rev.* **2010**, *62*, 1–96.

(25) Tran, T. A.; Rosik, D.; Abrahmsén, L.; Sandström, M.; Sjöberg, A.; Wällberg, H.; Ahlgren, S.; Orlova, A.; Tolmachev, V. Design, synthesis and biological evaluation of a HER2-specific affibody molecule for molecular imaging. *Eur. J. Nucl. Med. Mol. Imaging* **2009**, *36*, 1864–1873.

(26) Orlova, A.; Tolmachev, V.; Pehrson, R.; Lindborg, M.; Tran, T.; Sandström, M.; Nilsson, F. Y.; Wennborg, A.; Abrahmsén, L.; Feldwisch, J. Synthetic affibody molecules: a novel class of affinity ligands for molecular imaging of HER2-expressing malignant tumors. *Cancer Res.* **2007**, *67*, 2178–2186.

(27) Ahlgren, S.; Orlova, A.; Wällberg, H.; Hansson, M.; Sandström, M.; Lewsley, R.; Wennborg, A.; Abrahmsén, L.; Tolmachev, V.; Feldwisch, J. Targeting of HER2-expressing tumors using ^{111}In -ABY-025, a second-generation affibody molecule with a fundamentally reengineered scaffold. *J. Nucl. Med.* **2010**, *51*, 1131–1138.

(28) Wällberg, H.; Orlova, A.; Altai, M.; Hosseinimehr, S. J.; Widström, C.; Malmberg, J.; Ståhl, S.; Tolmachev, V. Molecular design and optimization of ^{99m}Tc -labeled recombinant Affibody molecules improves their biodistribution and imaging properties. *J. Nucl. Med.* **2011**, *52*, 461–469.

(29) Tolmachev, V.; Orlova, A. Influence of labelling methods on biodistribution and imaging properties of radiolabelled peptides for visualisation of molecular therapeutic targets. *Curr. Med. Chem.* **2010**, *17*, 2636–55.

(30) Pascal, R. R. Renal manifestations of extrarenal neoplasms. *Hum. Pathol.* **1980**, *11*, 7–17.

(31) Abrams, H. L.; Spiro, R.; Goldstein, N. Metastases in carcinoma; analysis of 1000 autopsied cases. *Cancer* **1950**, *3*, 74–85.

(32) Decristoforo, C.; Mather, S. J. ^{99m}Tc -Technetium-labelled peptide-HYNIC conjugates: effects of lipophilicity and stability on biodistribution. *Nucl. Med. Biol.* **1999**, *26*, 389–396.

(33) George, A. J.; Jamar, F.; Tai, M. S.; Heelan, B. T.; Adams, G. P.; McCartney, J. E.; Houston, L. L.; Weiner, L. M.; Oppermann, H.; Peters, A. M. Radiometal labeling of recombinant proteins by a genetically engineered minimal chelation site: technetium- ^{99m}Tc coordination by single-chain Fv antibody fusion proteins through a C-terminal cysteinyl peptide. *Proc. Natl. Acad. Sci. U.S.A.* **1995**, *92*, 8358–8362.

(34) Francesconi, L. C.; Zheng, Y.; Bartis, J.; Blumenstein, M.; Costello, C.; De Rosch, M. A. Preparation and characterization of $[^{99m}\text{TcO}]$ apcitide: a technetium labeled peptide. *Inorg. Chem.* **2004**, *43*, 2867–2875.

(35) Cyr, J. E.; Pearson, D. A.; Wilson, D. M.; Nelson, C. A.; Guaraldi, M.; Azure, M. T.; Lister-James, J.; Dinkelborg, L. M.; Dean, R. T. Somatostatin receptor-binding peptides suitable for tumor radiotherapy with Re-188 or Re-186. Chemistry and initial biological studies. *J. Med. Chem.* **2007**, *50*, 1354–1364.

(36) Wällberg, H.; Ahlgren, S.; Widström, C.; Orlova, A. Evaluation of the radiocobalt-labeled $[\text{MMA-}^{60}\text{Co-DOTA-Cys61}]$ -Z HER2:2395(-Cys) Affibody molecule for targeting of HER2-expressing tumors. *Mol. Imaging Biol.* **2010**, *12*, 54–62.

(37) Tolmachev, V.; Velikyan, V.; Sandström, M.; Orlova, A. A HER2-binding Affibody molecule labeled with ^{68}Ga for PET imaging. Direct in vivo comparison with ^{111}In -labelled analogue. *Eur. J. Nucl. Med. Mol. Imaging* **2010**, *37*, 1356–1367.

(38) Mume, E.; Orlova, A.; Larsson, B.; Nilsson, A. S.; Nilsson, F. Y.; Sjöberg, S.; Tolmachev, V. Evaluation of ((4-hydroxyphenyl)ethyl)-maleimide for site-specific radiobromination of anti-HER2 affibody. *Bioconjugate Chem.* **2005**, *16*, 1547–1555.

(39) Kramer-Marek, G.; Kiesewetter, D. O.; Martiniova, L.; Jagoda, E.; Lee, S. B.; Capala, J. $[^{18}\text{F}]$ FBEM-Z_{HER2:342}-Affibody molecule, a new molecular tracer for in vivo monitoring of HER2 expression by positron emission tomography. *Eur. J. Nucl. Med. Mol. Imaging* **2008**, *35*, 1008–1018.

(40) Lundberg, E.; Brismar, H.; Gräslund, T. Selection and characterization of Affibody ligands to the transcription factor c-Jun. *Biotechnol. Appl. Biochem.* **2009**, *52*, 17–27.